Available online at www.sciencedirect.com
SCIENCE DIRECT®
ELSEVIER
Deep-Sea Research I 52 (2005) 137–160
DEEP-SEA RESEARCH
PART I
www.elsevier.com/locate/dsr

North Brazil current rings viewed by TRMM Microwave Imager SST and the influence of the Amazon Plume

Amy Ffield*

Earth and Space Research, 290 Clausland Mountain Road, Upper Grandview, NY 10960-4113, USA

Received 20 June 2003; received in revised form 14 May 2004; accepted 20 May 2004
Available online 5 November 2004

Abstract

In the western equatorial Atlantic, 5 years of satellite Sea Surface Temperature (SST) measurements (1998–2002) from the cloud penetrating Tropical Rainfall Measuring Mission (TRMM) Microwave Imager reveal SST signatures of rings shedding from the North Brazil Current (NBC) as it separates from the South American coastline north of the Amazon River Delta and retroflects eastward between 5 and 10°N. By removing the spatial-mean SST from a 7° by 7° square of the nearly instantaneous measurements of each satellite pass, the 46.7 day aliasing period of the diurnal solar cycle is reduced, and seven to eight rings are observed per year with relatively warm (cold) SST anomalies of up to 1 °C in the first (second) half of the year. The sense of the SST anomalies carried by the NBC rings are determined by the contrast between the NBC SST and the regional SSTs that are influenced by the far-reaching seasonally varying Amazon River freshwater plume. Within a 1.6-year period, 12 of the SST anomalies are validated by in situ mooring array data confirming the predicted sense of the SST anomalies for each season. According to historical hydrographic data, during the first half of the year, the Amazon Plume is generally contained northwest along the coast, whereas during the second half of the year, the Amazon Plume surrounds the NBC retroflection on the west and the north, and from the surface down to 50 m, imposing a dramatic surface salinity contrast up to −4 and a surface temperature contrast up to +2 °C across the front. The surface layer characteristics of the rings shed from the NBC retroflection reveal varying influence of the Amazon Plume. Of the four rings surveyed in the NBCR experiment, Amazon Plume water is found only on the edges of three surface-intensified rings, whereas it completely covers the surface layer of the one thermocline-intensified ring. The maximum current cores of the NBC and retroflection are observed within tens-of-meters of the edges of the Amazon Plume. As the fresher and typically warmer surface waters associated with the Amazon Plume are buoyant relative to the saltier and typically colder surface waters carried by the NBC, the varying position of the Amazon Plume may seasonally influence the surface dynamics in the region.
© 2004 Elsevier Ltd. All rights reserved.

Keywords: North Brazil current; Rings; Amazon Plume; TRMM; TMI; SST

*Tel.: +1 845 353 1733.
E-mail address: ffield@esr.org (A. Ffield).

0967-0637/$ - see front matter © 2004 Elsevier Ltd. All rights reserved.
doi:10.1016/j.dsr.2004.05.013

1. Introduction

From its origin near the easternmost protrusion of the South American continent, the North Brazil Current (NBC) flows northwest alongside the Brazilian coast. It continually increases its transport with input of South Equatorial Current waters while becoming more surface-intensified (Stramma and Schott, 1996). After the NBC crosses the equator, it separates from the South American coast north of the Amazon River Delta and retroflects eastward between 5 and 10°N feeding the North Equatorial Countercurrent along with a smaller contribution from the North Equatorial Current (Wilson et al., 1994). At the retroflection anticyclonic rings are shed and translate northwestwards towards the Caribbean significantly contributing to the cross-equatorial transfer of warm South Atlantic upper-ocean water to the North Atlantic (most recently, Fratantoni and Glickson, 2002; Garraffo et al., 2003; Garzoli et al., 2003; Goni and Johns, 2003; Johns et al., 2003). This warm upper-layer transfer is required to balance the cold and deep southward export of 15 ± 2 Sv ($1\,\mathrm{Sv} = 1 \times 10^6\,\mathrm{m}^3/\mathrm{s}^{-1}$) net production of North Atlantic Deep Water (Ganachaud and Wunsch, 2000).

Modern, more varied types of measurements, as well as higher spatial and temporal resolution of the observations, enable the presence of the translating NBC rings to be detected. However, historically the northwestward flow in the area was called the Guyana Current, and it was interpreted as an extension of the South Equatorial Current and defined as a broad northwestward flow from the vicinity of the Amazon River mouth to the Caribbean (Metcalf, 1968). Recent shipboard hydrographic and current measurements confirm that NBC rings are large, with diameters up to 400 km (Wilson et al., 2002). The NBC rings are frequent, with an array of inverted echo sounder mooring observations revealing a continually retroflecting NBC and seven to eight rings shedding over 12-month time periods (Garzoli et al., 2003, 2004), and the 1/12 degree Miami Isopycnic Coordinate Ocean Model producing a ring shedding rate of 8.3 rings per year (Garraffo et al., 2003). Also, observations from a current meter mooring indicate that the NBC rings are seemingly slow, taking about 1 month for the leading and trailing edges to pass across a longitude with an average 12.5 km per day translation speed (Johns et al., 2003). Therefore, historically, it is probable that the mean translating signatures of the individual NBC rings merged with each other to appear as a unified broad flow. Nonetheless, the near-equatorial region is complex and variable, and the different pathways are certainly not unambiguously known. In particular, simply substituting "translating rings" for the previous description of the "Guyana Current" may be premature, as there is some evidence indicating the possibility of a coastal component of the NBC that does not retroflect and does not detach as a ring, but that continues towards the Caribbean as a more-or-less steady coastal current (Schott et al., 1998; Johns et al., 1998; Bourlès et al., 1999).

Theory supports the presence of the NBC rings, as it is shown that the momentum flux of the approaching and retroflecting NBC can only be balanced by anticyclonic rings forming, shedding, and drifting to the west (Nof, 1996; Nof and Pichevin, 1996). Several studies associate Rossby waves with NBC rings. Forty to sixty-day variability in current observations from three moorings deployed in 1987–1988 in the region were related to NBC rings and consistent with a description of baroclinic Rossby waves (Johns et al., 1990). Theoretically when long Rossby waves reflect at the western boundary creating short Rossby waves, the interaction with the coastal boundary and the beta effect causes vorticity anomalies to detach and propagate northwestward along the coast (Ma, 1996). A high resolution general circulation model shows that the NECC is barotropically unstable and that it radiates Rossby waves with a period of 63 days (steady winds) or 50 days (variable ones) that reflect at the Brazilian coast producing NBC rings (Jochum and Malanotte-Rizzoli, 2003).

In order to study the mechanisms which contribute to NBC ring formation and the structure and dynamics of the rings themselves, the North Brazil Current Rings (NBCR) experiment was conducted (Fratantoni and Glickson, 2002; Garraffo et al., 2003; Garzoli et al., 2003,

2004; Goni and Johns, 2003; Johns et al., 2003). The multi-institutional field program began in November 1998 and ended in June 2000, creating the most comprehensive suite of NBC retroflection and rings observations to date. The results from the current meter mooring (Johns et al., 2003) and the inverted echo sounder array (Garzoli et al., 2003) reveal seven rings shedding from the NBC in 1999. These results are complemented by the analyses of remotely sensed altimetry (Goni and Johns, 2003) and ocean color (Fratantoni and Glickson, 2002) data, each study easily and clearly identifying a different set of five of the seven rings observed in 1999. Both remote sensing studies have suggestions of additional rings, with weak sea height signals in altimetry, possibly indicating subsurface rings, and an additional two rings detected downstream (but not in the formation region) in ocean color. Remote sensing is an obvious way to continue to monitor the shedding of NBC rings, because the observational systems are already in operation. However, in order to provide continuous and accurate estimates, the advantages and deficiencies of each measurement need to be recognized: altimetry reveals the spatial and temporal pattern of the regional sea surface height of the ocean, but the elevated sea surface signature of the NBC rings may be occasionally masked due to a local steric effect (Goni and Johns, 2003); ocean color reveals a clear visualization of the rings, but the NBC rings can possibly be missed due to the seasonality in the source of the signal—the Amazon River (Fratantoni and Glickson, 2002).

To date, remotely measured Sea Surface Temperature (SST) has not been used to identify NBC rings. Here, 5 years of satellite SST observations from the cloud penetrating Tropical Rainfall Measuring Mission (TRMM) Microwave Imager are analyzed to see if NBC rings have a detectable SST signature and to identify possible unique contributions to the study of NBC rings using SST.

2. Data

The 5 years of satellite TRMM Microwave Imager SST data used in this study begin in early December 1997 and continue to the end of January 2003. The advantage of the TRMM Microwave Imager (Wentz and Meissner, 2000) is its ability to penetrate clouds, whereas the more traditional infrared-based satellite SST measurements are blocked by cloud cover. (Ocean color measurements are blocked by clouds as well.) The 0.25° by 0.25° gridded, Version-3, TRMM data set daily files were obtained from the www.ssmi.com web site. In general there is at least one measurement listed every 3 days at each grid point, and often there are two measurements listed per day at each grid point. Satellite sampling limitations are addressed in the data analysis sections. According to the web site the microwave measurements are sensitive to the sea surface roughness, and "A primary function of the TRMM SST retrieval algorithm is the removal of surface roughness effects". The main results of this study do not depend on the absolute accuracy of the TRMM SST measurements, but on their relative differences (which may be adversely affected by surface roughness effects keyed to the wind field) and longer period variability. Within the context of this study, it is estimated that the TRMM results are useful at SST differences of 0.2 °C and greater. In the analysis, a single comparison is made between the TRMM microwave-based SST to an infrared-based SST product, the 7-day averaged Reynolds optimal interpolation SST, provided by the NOAA-CIRES Climate Diagnostics Center (Boulder, Colorado, USA, www.cdc.noaa.gov). A small subset of the hydrographic and velocity data from one of cruises of the NBCR experiment and the regional historical hydrographic data from the National Oceanographic Data Center (NODC), released in 2002, are used in the latter part of the paper to study the Amazon Plume.

In order to easily compare results with other studies, rings identified by the TRMM SST observations, which span many years, are named as follows: TMI-yy-##, where TMI represents TRMM Microwave Imager, yy represents the last two digits of the year, and ## represents the number of the rings observed so far in that year, e.g. TMI-99-6 is the sixth ring observed in 1999 by

the satellite SST measurements. NBC rings cited from published literature are prefixed by the observing instrument type and suffixed with the identifier used in that publication; for example, for the results from the NBCR experiment, the Current Meter observations (Johns et al., 2003) are listed here as CM-1, and so on.

3. Analysis

3.1. Identifying NBC rings using SST

Two SST images are presented to demonstrate the capability of the remotely sensed SST measurements to detect NBC rings despite small SST gradients. In addition, the SST signatures of the NBC and ring translation corridor are interpreted to explain the observed seasonal changes in temperature gradients.

3.1.1. A NBC ring with relatively cold SST

A 5-day average of SST centered on October 4, 1999 is shown in Fig. 1. The locations of the instruments from the NBCR experiment are indicated, and they are included in order to enable direct comparisons with published NBCR experiment results. In Fig. 1, the NBC is clearly revealed in the SST image, moving northwest along the coast, sweeping between the pressure gauge (PG) and inverted echo sounder 17, then retroflecting, and returning between the two inverted echo sounders located just to the northeast (16 and 14). Garzoli et al. (2004) use these four instruments to estimate the variability in the transport of the NBC and its retroflection, along with shipboard Acoustic Doppler Current Profiler measurements to validate the results; at this date, October 4, 1999, the northwestward flowing NBC and the southeastward flowing retroflection are estimated to have an energetic 20 Sv transport in the upper

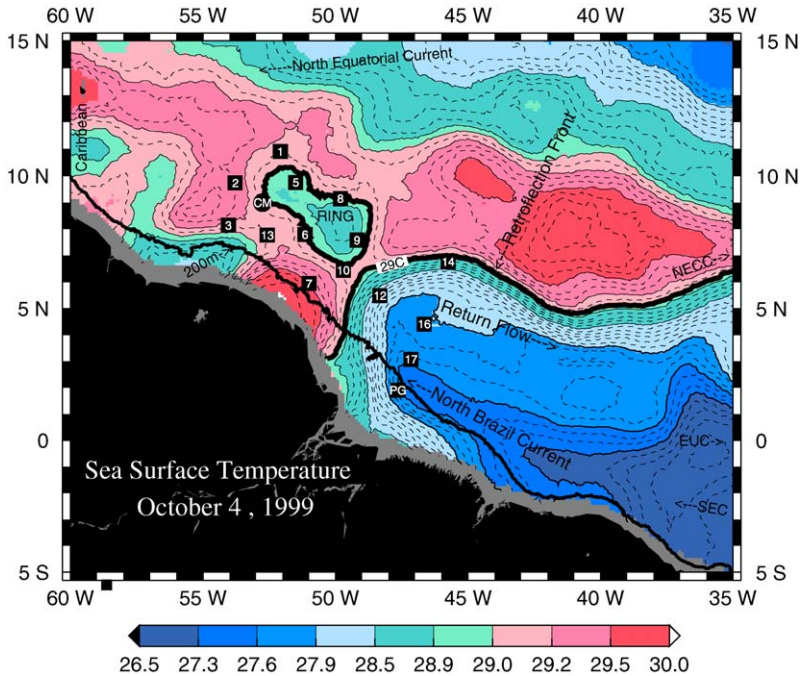

Fig. 1. The SST image for October 4, 1999 in the region of the NBC; 5 days of data have been averaged to construct the image smoothed by a 1° by 1° block average. The positions of the inverted echo sounders (numbers), current meter mooring (CM), and shallow pressure gauge (PG) from the NBCR experiment are shown. A ring with relatively cool SST is observed near the location of the CM. Generalized locations of some upper ocean currents are indicated with abbreviations as follows: North Equatorial Countercurrent (NECC), Equatorial Undercurrent (EUC), and South Equatorial Current (SEC).

300 m. The SST front between the NBC and the surrounding waters is sharply delimited by the 29.0 °C contour that encloses a 150 km wide band with a 1.0 °C temperature drop. In addition, a NBC ring is observed in the SST image to have recently pinched off from the retroflection carrying the same relatively cool surface waters as the NBC. At this date the core of the NBC is around 27.5 °C (between PG and 17), which is more than 1.5 °C cooler than the 29.0–29.5 °C surface waters to the northwest within the ring translation corridor. The contrast in the SST between the core of the ring and the surrounding water is 0.3–0.4 °C. This ring (TMI-99-6) is well documented by the NBCR experiment, identified in the ocean color (SW-J, Fratantoni and Glickson, 2002), current meter mooring (CM-7, Johns et al., 2003), and inverted echo sounder mooring (IES-8, Garzoli et al., 2003) results. Altimeter results that overlap with the NBCR experiment time period do not detail individual rings (Goni and Johns, 2003), so while a one-to-one comparison can not be made, the rings identified by altimeter are reported to agree with the NBCR experiment ring identifications (Goni, personal communication).

The most surprising observation here is the clear visual image of the NBC pathway in SST. An unanticipated observation is that the SST of the NBC and of the recently shed ring is colder than the surrounding waters, whereas the literature (including this study) refers to the relatively warm South Atlantic waters carried into the region by the NBC. These conflicting temperature descriptions can be reconciled by noting that probably just the near-surface is relatively cold, as discussed below, and that the deeper layers, which contain the bulk of NBC ring volumes, are relatively warm.

3.1.2. SST temperature contrast in the NBC region

After studying the SST data set to explore its potential for identifying NBC rings, it was concluded that the interplay between two opposing annual SST cycles must be carefully considered. It became evident that the NBC carries the SST signal from south of the equator, and then sheds a ring into a region north of the equator, characterized by an annual cycle opposite to its own. Therefore, it is the relative contrast in temperature, as a function of season that determines the surface temperature signature carried by the NBC rings. The smoothed SST records (Fig. 2c) from the main pathway of the NBC (47.25°W, 2.00°N) and from the location of the NBCR experiment current meter mooring (53°W, 9°N) illustrate how the NBC carries relatively warm (cold) surface water into a relatively cold (warm) region from about January–June (July–December). This seasonal cycle changes sign (warm versus cold) at dates that can differ by about 1 month depending on the individual year. The temperature contrast is as large as 1 °C in the first half of the year, and as large as 2 °C is the last half of the year in the smoothed records (Fig. 2b). (The SST time series in the NBC ring corridor, of course, includes the SST signal of the NBC rings as they pass through that location, so the actual temperature contrast might be larger.)

It is of interest to note that this contrasting SST pattern is influenced by the Amazon River plume (Lentz, 1995). Pailler et al. (1999) map the freshwater barrier layer from the Amazon and Orinoco River plumes. The Amazon Plume extends furthest offshore during the late summer and fall, and is swept around, and north of, the NBC retroflection during this time of year. The barrier layer associated with the Amazon Plume can trap heat in the surface (0–30 m), and it is associated with warm SST anomalies (Pailler et al., 1999). These warm SST anomalies might contribute to the SST of the NBC appearing relatively cold in the second half of the year. It is also the Amazon Plume that enables NBC rings to be tracked in ocean color data, because the Amazon discharges water with a large ocean color signal that is entrained into the edges of the NBC delineating the NBC rings when they are shed (most recently, Fratantoni and Glickson, 2002).

3.1.3. A NBC ring with relatively warm SST

In Fig. 3, a 5-day average of SST centered on February 19, 1999 is shown, but it is not as easy to interpret as the October 1999 image (Fig. 1). Whereas the NBC retroflection is dramatically highlighted by a cold SST in October (Fig. 1), the February SST (Fig. 3) displays warmer SST in the

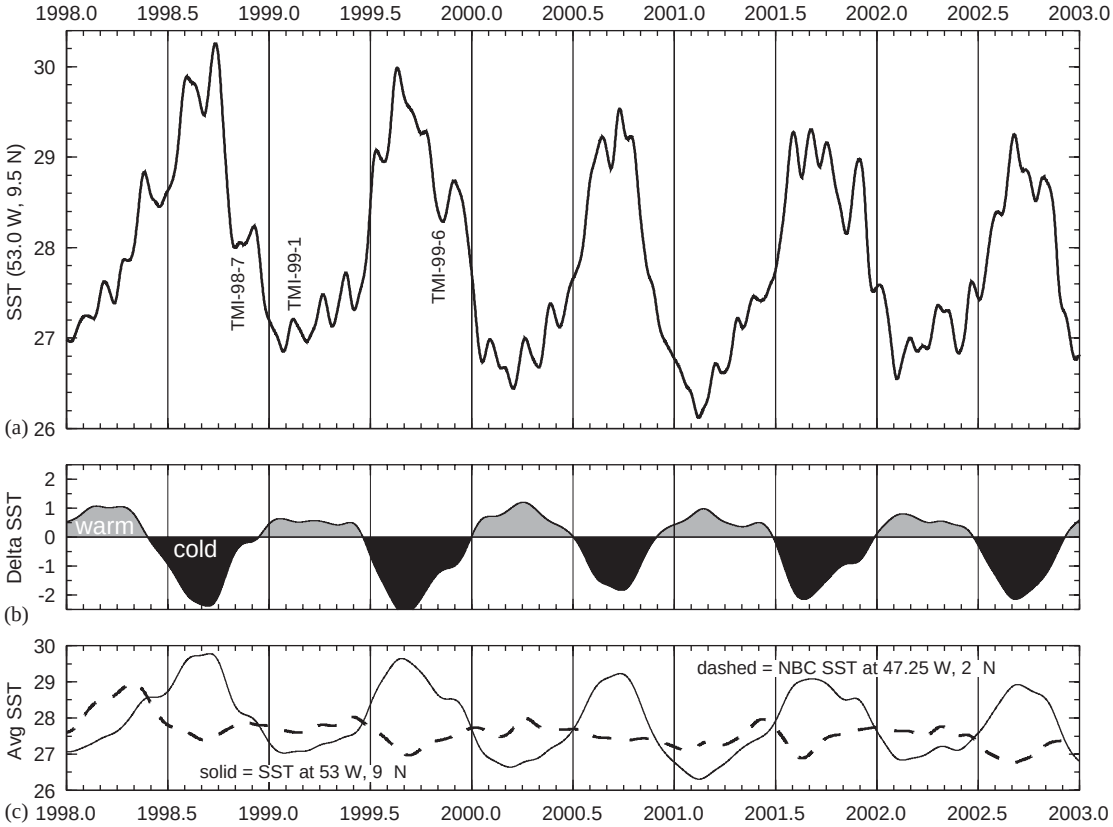

Fig. 2. (a) The time series of the SST at the location of the NBCR experiment current meter mooring (53°W, 9°N) smoothed by a 30-day Gaussian running mean. SST peaks with relative warm (cool) temperatures during the first (second) half of the year indicate possible NBC rings translating past the location. (b) The difference between the 90-day Gaussian filtered SST at the location of the current meter mooring and at the core of the NBC (47.25°W, 2.00°N) reveals whether NBC rings will carry relatively warm or cold SST. (c) The 90-day Gaussian filtered SST at the location of the current meter mooring and in the core of the NBC. (Each SST time series is an average of the four closest gridded time series in order to be centered over the chosen location.)

presumed path of the NBC between the PG and inverted echo sounder 17, but the SST contours do not reveal a clear image of the NBC pathway. The NBCR experiment pressure gauge was deployed after this date, so there is not an estimate of the northwestward flowing NBC. The retroflecting flow was measured revealing an estimated 18 Sv southeastward transport in the upper 300 m between IES16 and IES14 (Garzoli et al., 2004), but its signature is not apparent in the SST image. Possibly the SST in February is also indicative of a coastal current carrying warm water northwestward along the coast (Schott et al., 1998; Johns et al., 1998; Bourlès et al., 1999), warm water carried by earlier NBC rings, or a seasonal signature of the local SST that is obscuring a NBC signature. Nonetheless, a ring is observed in the February SST image with relatively warmer SST then the surrounding surface water. At this date, the NBC is 27.6 °C between the PG and inverted echo sounder 17, which is about 1.0 °C warmer than the surface waters surrounding the detached ring to the northwest. The ring observed in the February SST image (TMI-99-1) corresponds to the ring observed in the remotely sensed ocean color (SW-G, Fratantoni and Glickson, 2002) and altimeter (Goni and Johns, 2003) data and in the NBCR Experiment shipboard survey (Ring 3, Wilson et

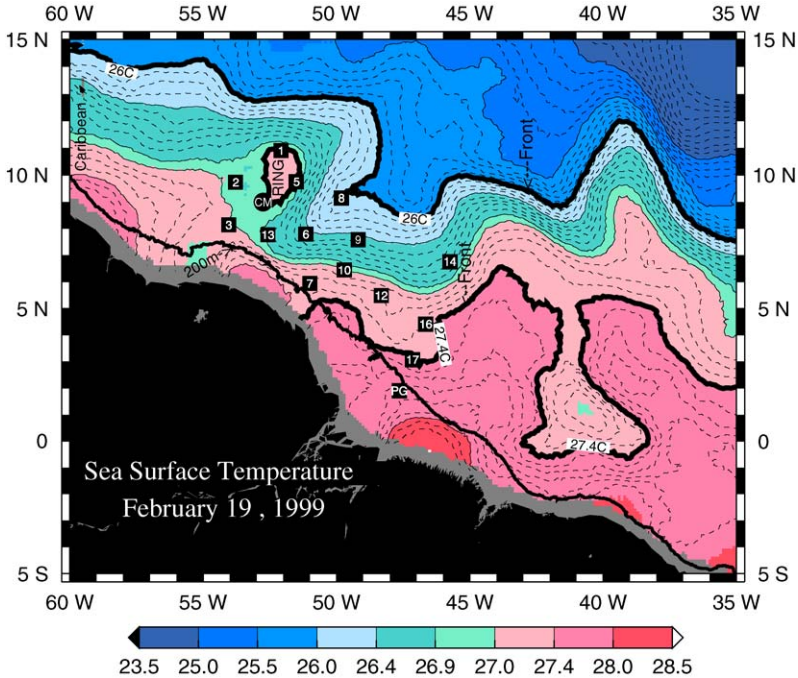

Fig. 3. The SST image for February 19, 1999 in the region of the NBC; 5 days of data have been averaged to construct the image smoothed by a 1° by 1° block average. The positions of the inverted echo sounders (numbers), current meter mooring (CM), and shallow pressure gauge (PG) from the NBCR experiment are shown. A ring with relatively warm SST is observed near the location of the CM.

al., 2002) and current meter (CM-2, Johns et al., 2003) and inverted echo sounder (IES-3, Garzoli et al., 2003) data.

3.2. Identifying NBC rings within SST time series

The previously discussed relatively cold SST (TMI-99-6) and warm SST (TMI-99-1) rings can also be identified as relative peaks within a SST time series (Fig. 2a). The SST time series chosen to present here is from the same location as the NBCR experiment current meter mooring deployment: 53°W, 9°N; the location of the time series is within the NBC ring corridor, and it is northwest of the NBC retroflection where the rings are shed. In 1999, three relatively warm peaks are prominent during the first half of the year, and three relatively cold peaks are evident in the second half of the year in the 30-day Gaussian filtered time series. These peaks may correspond to six of the seven rings observed in situ during 1999 in the NBCR experiment. However, in general, three physical factors may obscure detection of the rings in SST. First, near January and June, the contrast between the opposing annual SST cycles disappears as the temperatures from both cycles converge towards 28 °C before diverging again. Without a sharp temperature contrast between the SST in the NBC and ring translation corridor during those time periods, it is difficult or impossible to identify rings in SST. Second, a thermocline-intensified ring with low surface velocities, as observed in the first shipboard survey of the NBCR experiment (Wilson et al., 2002), may not carry surface NBC water, and therefore might not carry a SST signature. And third, after a ring is shed, subsequent forces (wind, local solar heating, mixing) may mask or obliterate the SST signature of the ring. In addition, satellite sampling limitations are also a potential problem due to aliasing of the diurnal solar heating cycle; this error is addressed below.

3.3. SST root-mean-square maps and aliasing of the diurnal solar heating cycle

In order to help assess the SST characteristics in the region, the Root-Mean-Square (RMS) of the SST time series (Fig. 4) at each grid location and of the 30–90-day SST anomaly time series (Fig. 5) at each grid location are calculated. The RMS calculations have the advantage that they are insensitive to geographical phase differences.

The geographical pattern of the SST time series RMS clearly shows a surface signature of the NBC penetrating northwestwards into the region (Fig. 4). The RMS is low in the region (less than 1 °C and generally south of 8°S) associated with the NBC and its retroflection, and is high in the region (greater than 1.1 °C and generally north of 8°S) associated with the North Equatorial Counter Current (NECC) and the North Equatorial Current (NEC). In essence, the RMS seems to reveal the smaller range in the annual cycle of the SST in the NBC, as compared to the more poleward NECC and NEC flows.

The geographical pattern of the 30–90-day anomaly SST time series RMS (Fig. 5) displays a more striking pattern of very low values (less than 0.2 °C) in the core pathway of the NBC, contained within 4° of the coast as it travels northwest, and as it retroflects around 50°W, 4°N and passes eastward. Medium RMS values (0.20–0.24 °C) are in the NECC pathway beginning at 35°W, 8°N, and extending all the way west to the coastal boundary between two massive, submarine promontories in the bathymetry, the Guiana Plateau and the Amazonas Cone. The highest values, by far (between 0.26 and 0.75 °C), are found along the coast at the coastal limit of the satellite coverage. However, examination of the SST time series at the location with the highest anomaly RMS value (0.75 °C at 49.375°W, 1.125°N next to the 0.65 °C contour in Fig. 5), exposes the aliasing of the diurnal solar heating cycle due to the satellite sampling limitations: the time series (not shown) is dominated by a 1.8 °C peak-to-peak oscillation with a period of 46.7 days. While there is typically a SST measurement at least once every 3 days in

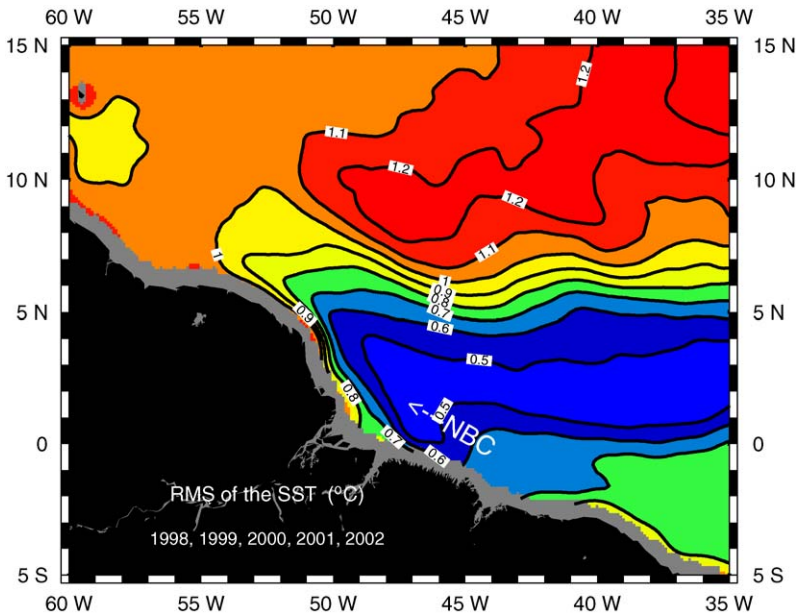

Fig. 4. The RMS of the 30-day Gaussian filtered SST at each 0.25° by 0.25° grid location for the 5-year time period smoothed by a 1° by 1° block average. The NBC is revealed as the lowest RMS values in the region, extending all the way to 55°W, which is associated with the maximum northwestward position of the NBC retroflection.

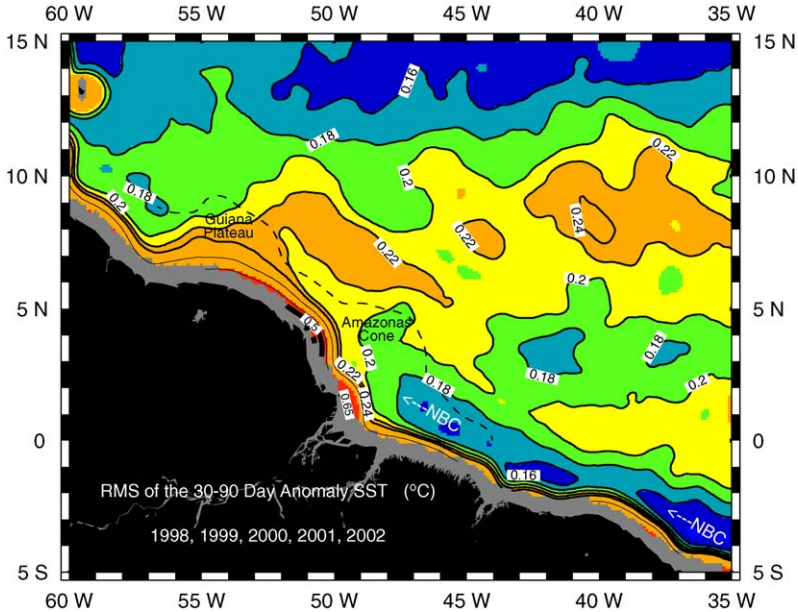

Fig. 5. The RMS of the 30–90-day Gaussian anomaly SST at each 0.25° by 0.25° grid location for the 5-year period smoothed by a 1° by 1° block average. In this bandwidth, the NBC is revealed as the lowest RMS values (as in Fig. 4), but in this case its signature only extends to 49°W. The highest RMS values (0.50–0.65 °C) are found in a narrow band along the coast (red shading), but examination of these time series expose that the signal is due to aliasing of the solar diurnal cycle into the SST record.

the TRMM data at each grid point, it actually takes about 46.7 days to repeat a measurement at approximately the same time-of-day due to the orbit of the satellite. Therefore, the diurnal SST cycle is manifested within the SST time series as a 46.7 day signal. The anomaly RMS map suggests that the highest aliasing (and therefore the largest diurnal cycles) are contained along the coast. But of course, even the aliasing of a relatively small diurnal cycle offshore may interfere with analysis of a relatively small SST signal of interest. The diurnal aliasing is particularly troubling because the 46.7 day alias period is within the range of NBC ring shedding rates. For example, when the results from the NBCR experiment inverted echo sounder array (Garzoli et al., 2003) and current meter mooring (Johns et al., 2003) are characterized in a histogram (not shown) by the number of days between shedding events for the 1.6 year observation period, the most typical shedding rate is around 45–55 days, with an average rate of 49.4 days and median rate of 49.3 days.

3.4. Removing the SST diurnal cycle

A simple technique is employed to reduce the aliasing of the solar diurnal cycle in the TRMM SST data. As the satellite passes over a region, a 7° wide swath of measurements is obtained. In one day, there might be two passes over a region of interest. In Fig. 6 the satellite swath pattern for one day is shown; of the two swaths intersecting 50°W, 10°N, one swath is from 12.2 h, and the other swath from 22.0 h (e.g. 10:00 p.m.). Because the observations obtained within each swath are essentially instantaneous as the satellite passes overhead, the individual swath image itself is not biased. This fact can be exploited. If the satellite pass is centered over the location of interest (by requiring 75% coverage within a 7° by 7° centered square), then the spatial-mean SST of the measurements within the square is removed from each measurement. By removing a constant value from the square, the geographical pattern is not changed, but the values are now SST anomalies.

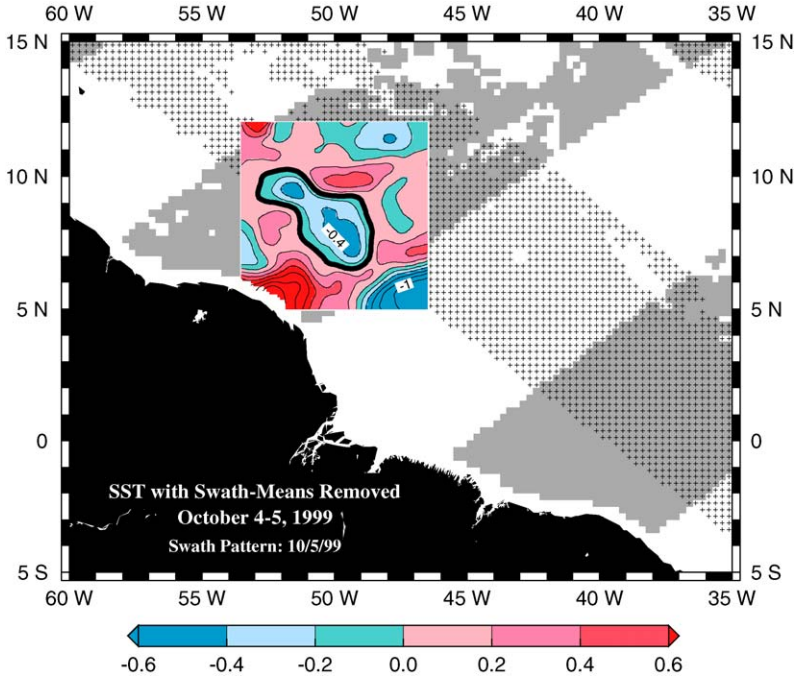

Fig. 6. The anomaly SST image for October 4–5, 1999 smoothed by a 1° by 1° block average; the swath-mean temperature has been removed from each swath and the results averaged together to re-construct the image. The swath sampling pattern for one day is shown in the background.

Away from the coastline—to a first-order approximation—this effectively removes most of the seasonal and diurnal SST signals from the swath, because those signals are expected to have a relatively spatially similar SST over a 7° by 7° square. However, a ring is likely to have a considerably spatially varying signal, with SSTs carried from the NBC retroflection region enclosed within a circular area of less than 4° diameter displaying extreme ring center or velocity core SST values, in contrast to surrounding generally constant "ambient" SSTs. For early October 1999, four swaths from over 2 days, with the individual swath-mean temperatures removed, are averaged together to re-construct the SST image (Fig. 6). The new representation of the cold SST ring (TMI-99-6), which is now a relatively unbiased anomaly image, compares well to the original image of the same cold SST ring (Fig. 1) that was a simple average of the data. The same swath-mean removal technique is used for the February 1999 warm SST ring (Fig. 7), and its anomaly signal also compares well to the simple average of the data (Fig. 3). These results suggest that the anomaly technique works well by preserving the spatially varying signal of the rings and that the original SST images themselves are probably not hopelessly biased by the solar diurnal cycle in comparison to the magnitude of the SST ring signal. This technique can also be used in other ocean regions where the SST features of interest have spatially varying SSTs within a relatively spatially uniform background SST field.

The swath-mean removal technique is carried out for the 5-year SST data set, and the resulting anomaly time series at the location of the NBCR experiment current meter mooring is extracted (Fig. 8). The anomaly time series displays the same relatively warm and cold peaks observed within the plain time series (Fig. 2a), and it reveals some additional anomalies as well. There are two benefits to the swath-mean removed anomaly time

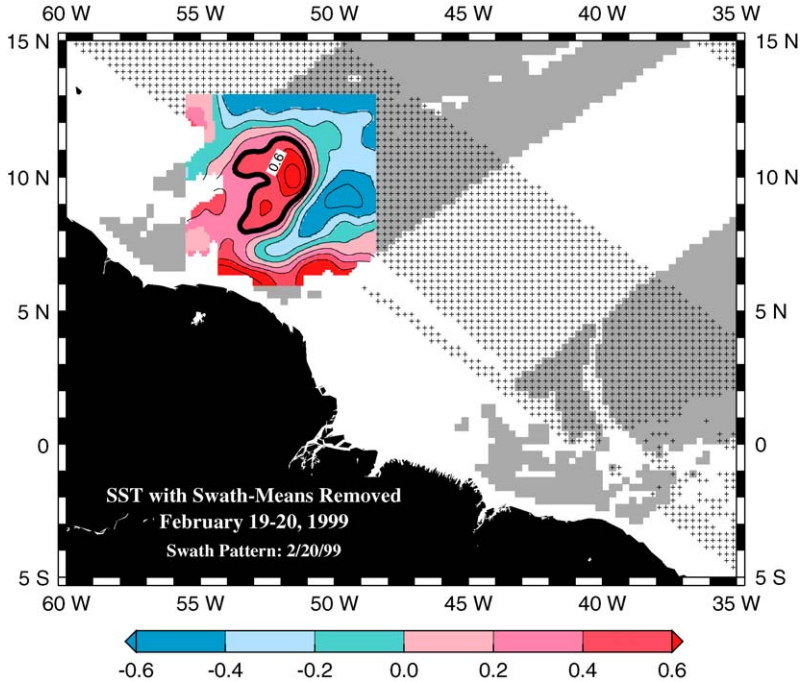

Fig. 7. The anomaly SST image for February 19–20, 1999 smoothed by a 1° by 1° block average; the swath-mean temperature has been removed from each swath and the results averaged together to re-construct the image. The swath sampling pattern for 1 day is shown in the background.

series: (1) diurnal aliasing is reduced; and (2) because the date that the SST contrast changes varies by a month or so each year around June–July and December–January (Fig. 2c), the technique avoids confusion at those time periods better exposing any ring anomalies passing by the location. In all, seven or eight anomalies are identified per year in the anomaly time series (Fig. 8a) that may indicate warm (cold) SST rings passing by the location in the first (second) half of the year. Time–longitude plots (not shown) suggest an average translation speed of these potential ring features around 14 km/day, similar to the ring translation speed estimates obtained in other NBC studies: 12.5 km/day from the current meter mooring results (Johns et al., 2003), 12.4 km/day from the inverted echo sounder moorings results (Garzoli et al., 2003), 13.0 km/day from ocean color results (Fratantoni and Glickson, 2002), and a range of 7.5–24 km/day from altimeter results (Goni and Johns, 2003).

3.5. Comparing NBC ring observations

When comparing the dates of NBC ring identifications obtained from different measurement techniques the results are in clear agreement most of the time, but in a few occasions a unified scenario is not obvious. Probably the apparent date of a ring shedding event, or the date when the ring passes a location, varies between measurement techniques for several physical reasons, in addition to any study-specific biases due to differing definitions, methods, and data type. The rings are large, often deep, and continually moving northwestward, and the different measurement techniques may first detect a ring signature anywhere within a considerable geographical and temporal span. There are single-point measurements (current meter) versus geographic array measurements (inverted echo sounder, remote sensing). While some measurements have temporal resolutions on the order of hours (current meter,

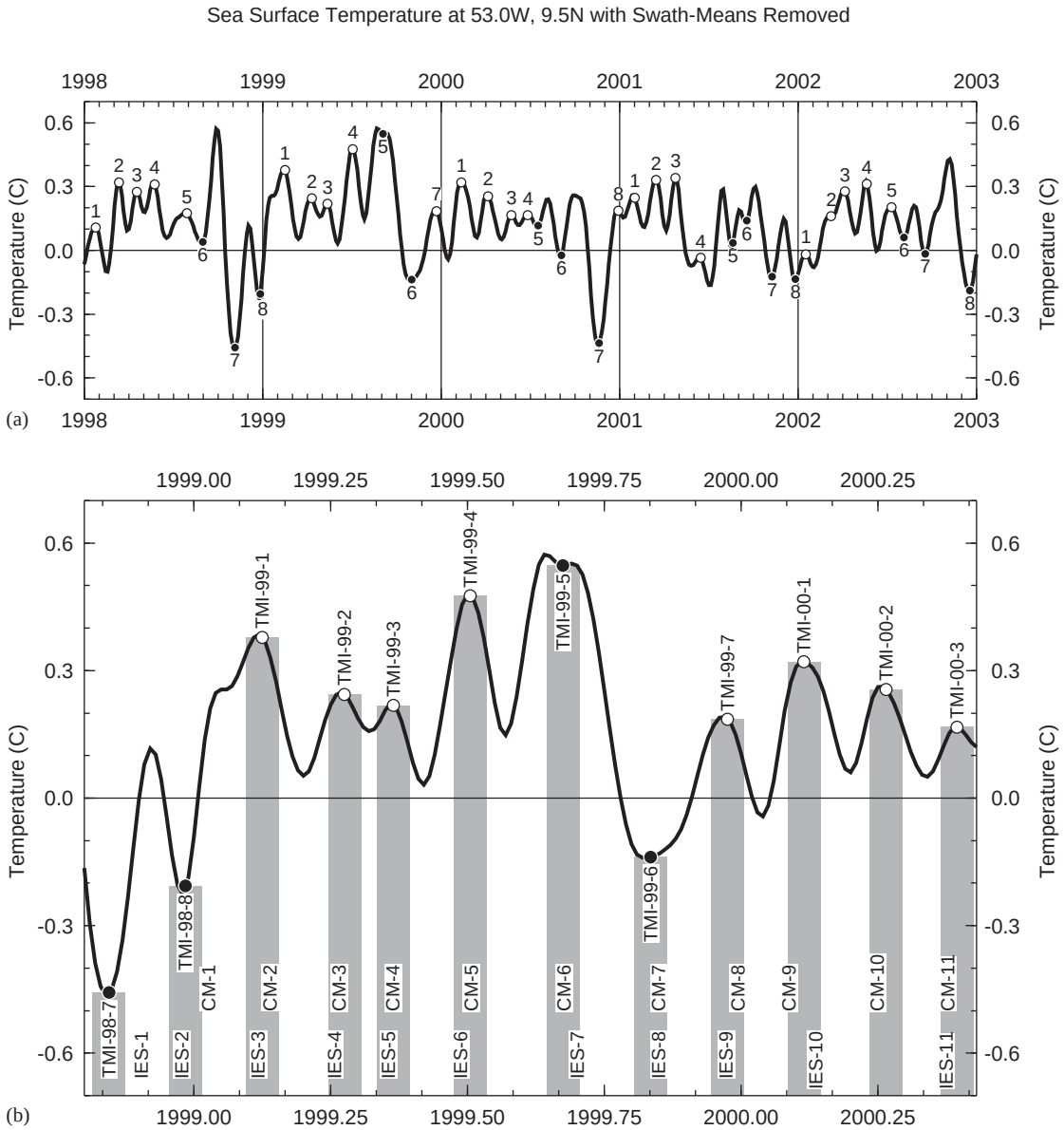

Fig. 8. (a) The individual swath-mean temperature is removed from each satellite pass to construct this anomaly SST time series at the location of the NBCR experiment current meter mooring (53°W, 9°N). The time series is smoothed by a 30-day Gaussian running mean. Possible NBC rings—as indicated by SST anomalies—are identified by open (solid) circles at the maximum (minimum) temperatures during the first (second) half of the year. (b) The anomaly time series is expanded for the 1.6 year time period of the NBCR experiment. The temporal correspondence between the SST anomalies and the in situ current meter and inverted echo sounder ring results is highlighted by gray bars centered on the SST anomalies.

inverted echo sounder), other measurements have temporal resolutions on order of days (remote sensing). The velocity fields suggest considerable timing variability with depth with distinct surface versus subsurface features (Johns et al., 2003). Therefore, the surface measurements (ocean color,

SST) will detect a different signal than measurements that integrate the upper layers (inverted echo sounder, altimeter).

Here, for the most robust evaluation, the SST anomaly results are compared to the in situ upper-layer current meter and inverted echo sounder results for the 1.6 year time period of the NBCR experiment (Fig. 8b). During this time period, the timing of the 12 observed SST anomalies directly correspond to the 12 in situ current meter and inverted echo sounder NBC ring results, confirming that the anomalies are indeed the SST signatures of NBC rings passing by the location and that any residual diurnal aliasing is less than the SST signal of the rings. The only apparent discrepancies are the rings identified at the very beginning of the inverted echo sounder record (November 1998, IES-1) and current meter record (December 1998–January 1999, CM-1), but these are easily resolved: (1) IES-1 was identified in the inverted echo sounder array when it was already downstream, because the array deployment finished after the ring shed; (2) while the current meter mooring (which began recording later than the inverted echo sounder array) suggests a January 1999 date for CM-1, the inverted echo sounder result for the same ring (IES-2) asserts a December 1998 date; and (3) in addition, during the overlapping in situ records, one ring was observed in the current meter mooring, CM-10, that was not observed in the inverted echo sounder array. The key achievement of the SST and in situ ring comparison is not the successful identification of NBC rings, as that can also be accomplished remotely with satellite ocean color and altimetry measurements, but that the timing of the rings observed in the NBCR experiment directly correlates to the timing of the warm (cold) SST anomalies during the first (second) half of the year as predicted (Fig. 8b, open circles indicate warm anomalies, solid circles indicate cold anomalies).

3.6. The Amazon River plume

The Amazon and Orinoco Rivers are significant in this region as they discharge almost 20% of the total annual global freshwater river outflow directly to the surface waters of the western equatorial Atlantic and Caribbean. The ~0.2 Sv freshwater discharge from the Amazon River is the world's largest, and the Amazon Plume is adjacent to the NBC ring generation region. While the ~0.03 Sv freshwater discharge from the Orinoco River is about the world's 4th largest (Perry et al., 1996), the Orinoco Plume is downstream of the NBC ring generation region.

Warm SST anomalies associated with the Amazon Plume's barrier layer (Pailler et al., 1999) may contribute to the temperature contrast between the NBC and the surrounding region that enables the NBC rings to be detected. Satellite SST data provide a complete spatial view of the surface temperature of the region, but at this date, there is not yet a similar product available to view the other dynamically important property, salinity. In order to better understand the role of the Amazon Plume in determining the surface layer characteristics of NBC rings, historical in situ hydrographic data are analyzed.

3.6.1. Seasonal cycle of the Amazon Plume

The seasonal cycle of the Amazon River's freshwater plume is characterized by determining the months in which the Amazon Plume completely encircles the NBC retroflection, reaching, not only to the west side of the retroflection, but all the way around to the north side of the retroflection. In order to make this characterization, the historical surface salinities for the region north of the typical position of the NBC retroflection, at the 5°N front (as observed in Fig. 1), and for the region within the NBC retroflection, for comparison, are averaged monthly (smoothed by a 1-month filter) to produce two mean-annual time series (Fig. 9). For the entire year the stations within the NBC retroflection (gray curve) display remarkably constant monthly averaged surface salinities between 35.9 and 36.2, characteristic of the South Atlantic water. North of the 5°N front (black curve), the monthly averaged salinities for November to June are also between 35.9 and 36.2, but from July–October very low values are observed due to the Amazon River freshwater plume encircling the NBC retroflection during this time of year; specifically, in August, the salinities

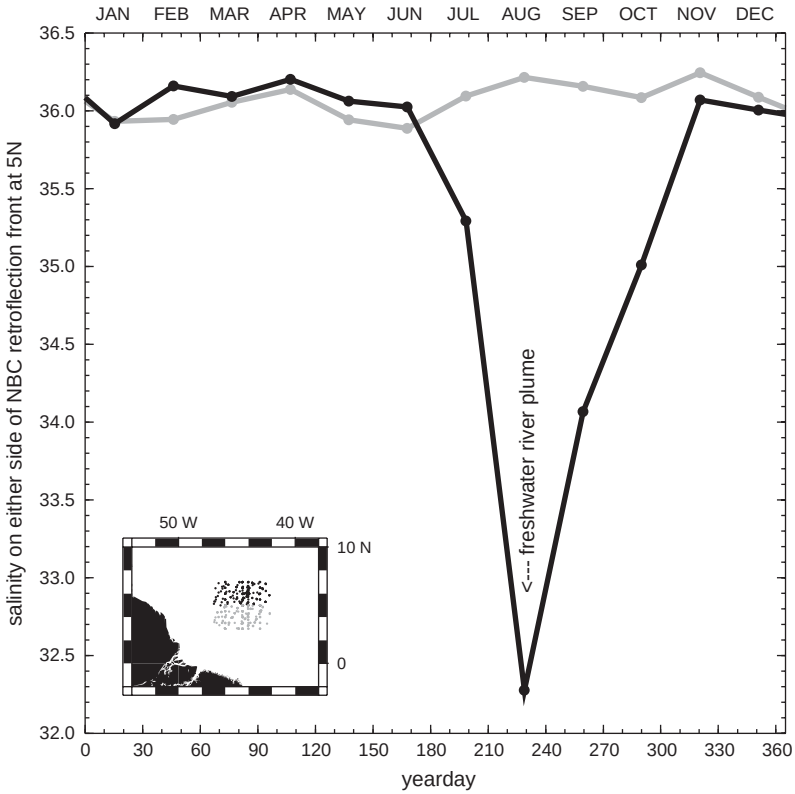

Fig. 9. The historical annual-mean surface salinity, smoothed by a 1-month block average, on either side of the NBC retroflection front revealing the dramatic arrival of the freshwater plume north of the retroflection in the second half of the year.

drop to almost 32, an impressive salinity difference of 4 across the front in this smoothed time series. The monthly Amazon River discharge has a minimum in November and a maximum in May and June (Hellweger and Gordon, 2002). Therefore, it is about a 2–3-month delay between the maximum in the Amazon River discharge and the minimum in the salinities observed north of the NBC retroflection. The time period that the low salinities of the Amazon Plume are observed north of the retroflection, July–October, is similar to the time period that the NBC rings display cold SST anomalies, July–December.

3.6.2. Geographic distribution of the Amazon Plume

To determine the seasonal geographical distribution of the Amazon low-salinity plume, salinity data from the January–June (first half of the year) and July–December (second half of the year) time periods are averaged (Fig. 10). These time periods sufficiently capture the two contrasting seasons observed in the surface salinity time series (Fig. 9), and they are the same as the two seasons identified in satellite SST (Fig. 2b). In the maps, the low salinity from the Amazon River freshwater plume generally flows to the northwest along the coast (Ou 1989) from January–June (Fig. 10a) until it reaches the eastern edge of the Guiana Plateau (52°W) whence it spreads broadly northwards. From July–December (Fig. 10b) the Amazon River freshwater signal also flows to the northwest along the coast, but then at the eastern edge of the Guiana Plateau it extends northward, and then both westwards (merging with the Orinoco Plume) and eastwards. The 35.4 salinity contour delineates

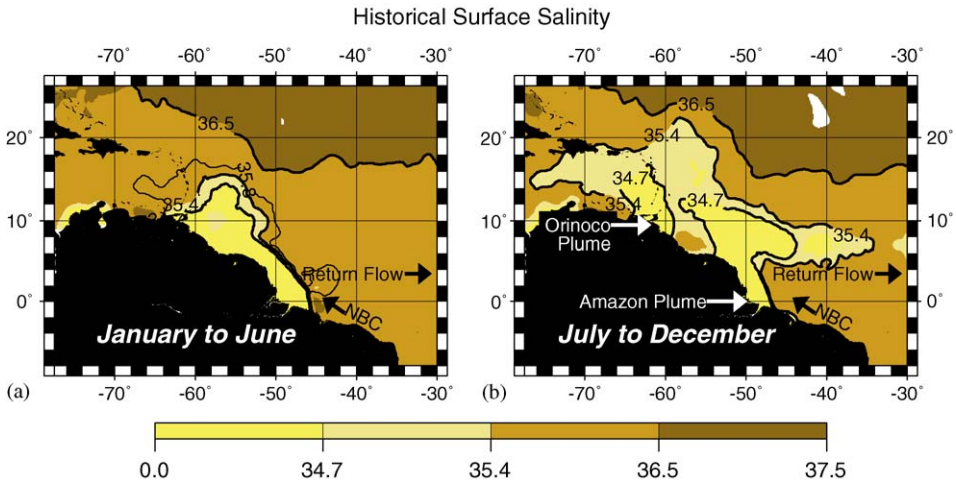

Fig. 10. The mapped historical surface salinity highlighting the Amazon and Orinoco River plumes smoothed by a 3° by 3° block average. During the July–December time period (b) the low-salinity plumes are far more geographically extensive than during the January–June time period (a). During July–December (b) the Amazon low-salinity plume wraps around the NBC and its retroflection, whereas during January–June (a) the Amazon low-salinity plume is only evident adjacent to the coast.

the eastward extent of the Amazon Plume as it spreads all the way to 34°W, 7°N, completely encircling the NBC retroflection. For the westward spreading of the plume, low salinities are observed entering the Caribbean; an earlier study found a very high inverse correlation ($R^2 = 0.92$) between the surface salinity (minimum of 34.24 in June; maximum of 35.48 in January) near Barbados (approximately located at 59°W, 13°N) and the 2-month lagged Amazon River discharge (Hellweger and Gordon, 2002). The spatial pattern of the July–December low surface salinity (Fig. 10b) is similar (as it necessarily should be) to the mapping of the river plume barrier layer for a similar time period (Pailler et al., 1999; their Fig. 5).

The geographic distribution of the historical surface temperature is also shown for completeness. During the July–December time period (Fig. 11b) when the Amazon low-salinity plume wraps around the retroflection, warm temperatures associated with the Orinoco and Amazon Plumes (Pailler et al., 1999) are visible. The warm temperatures of the Amazon Plume, reaching eastwards to 36°W, 7°N (Fig. 11b), can now be visually correlated to the low salinities of the Amazon Plume, reaching eastwards to essentially the same position, 34°W, 7°N (Fig. 10b). During the January–June time period (Fig. 11a) when the Amazon low-salinity plume is only evident adjacent to the coast (Fig. 10a), there is not an obvious temperature signature association with the river plumes. However, when only stations with surface salinities less than 32 are used (Fig. 12), relatively pure Amazon Plume water is isolated, and in both seasons the associated warm temperatures are now clearly spatially correlated to the low-salinity signature of the Amazon Plume confirming the connection (Fig. 10): During the January–June season (Fig. 12a), the highest temperatures (between 28 and 29.7 °C) are observed at the Amazon River mouth, and the lowest (between 27 and 25.4 °C) are observed downstream approaching the Caribbean as expected for a spreading plume continually subjected to dilution. During the July–December season (Fig. 12b), there is not a reduction in temperature with distance as in the other season (even if the temperature color scale is expanded), but the high temperatures (between 28 and 29.7 °C), now isolated to low-salinity river outflow, geographically confirm the seasonal pattern of the plume sweeping around the western and northern sides of the NBC retroflection. If a less-restrictive, higher salinity cutoff is used, then the Orinoco Plume is also visible.

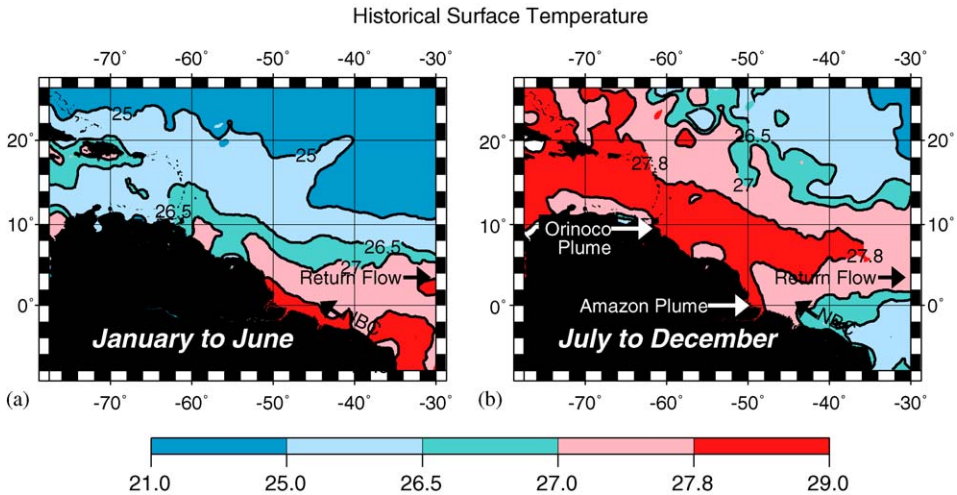

Fig. 11. The mapped historical surface temperature smoothed by a 3° by 3° block average. During the July–December time period (b) when the Amazon low-salinity plume wraps around the NBC and its retroflection (Fig. 10b), the warm temperatures associated with the Orinoco and Amazon Plumes (Pailler et al., 1999) are visible and the NBC is relatively cold. During the January–June time period (a) when the Amazon low-salinity plume is only evident adjacent to the coast (Fig. 10a), there is not an obvious temperature signature association with the Amazon and Orinoco Plumes and the NBC is relatively warm.

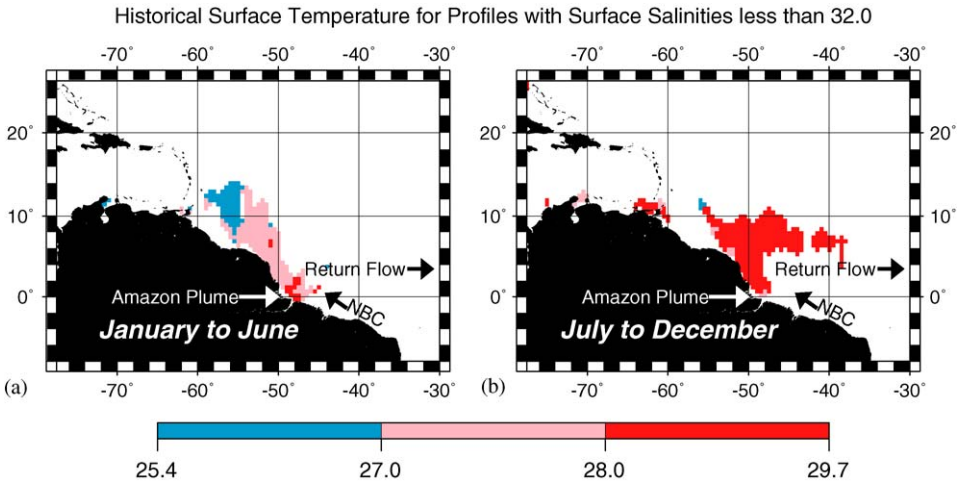

Fig. 12. The mapped historical surface temperature for only profiles with surface salinities less than 32 to isolate the low-salinity Amazon Plume, smoothed by a 2° by 2° block average. The spreading of the low-salinity Amazon Plume is associated with warm temperatures as noted in Pailler et al. (1999) in both the January–June (a) and July–December (b) time periods.

3.6.3. Depth of the Amazon Plume

To determine the depth of the Amazon Plume in the vicinity of the NBC retroflection, two hydrographic sections from April 1996 and September 1995 are examined. The data were selected from the NODC data set, and they are described in detail in Bourlès et al. (1999). In September 1995, the Amazon Plume can be identified by warm temperatures (Fig. 13b) and low salinities (Fig. 14b) north of 4°N, agreeing with the mapping of the surface salinity (Fig. 10b) when the Amazon Plume is observed to wrap around the NBC

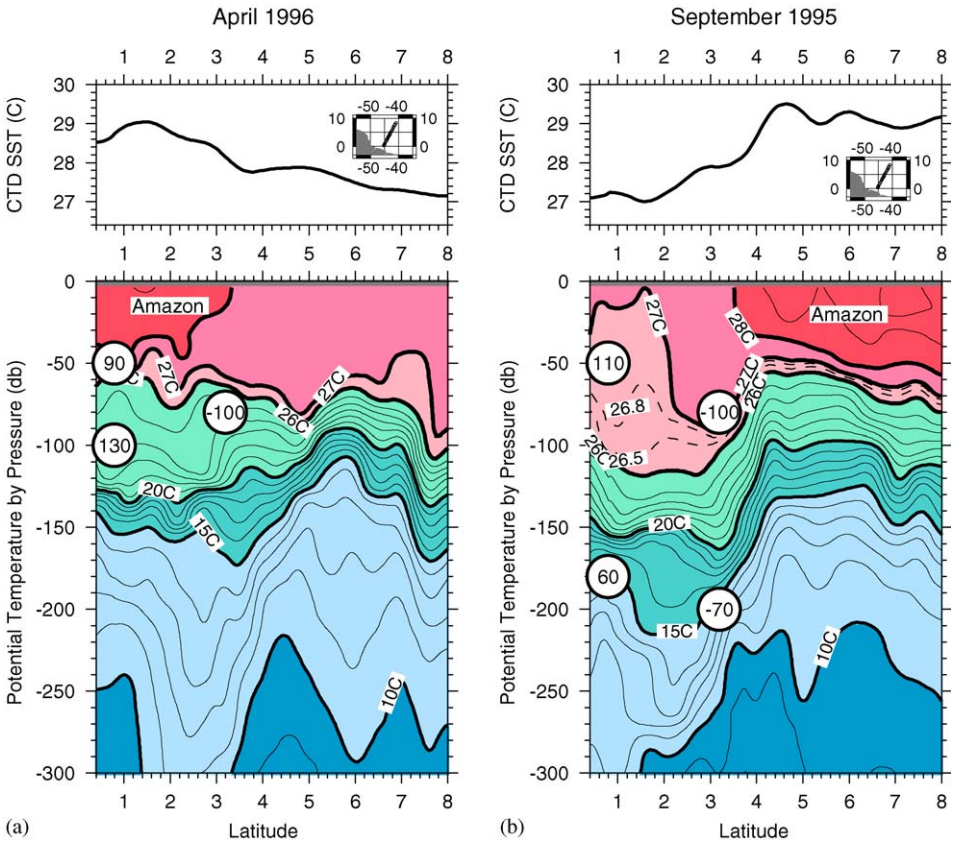

Fig. 13. Surface temperature–latitude plots and potential temperature–latitude sections for April 1996 (a) and September 1995 (b) obtained as part of the World Ocean Circulation Experiment (described in Bourlès et al., 1999). The locations of the stations are shown in the map insets, crossing the NBC and its retroflection. The warm temperatures of the Amazon Plume are indicated by the "Amazon" labels. In addition, the magnitude and depth of the NBC retroflection current cores (cm/s), obtained from acoustic doppler current measurements (Bourlès et al., 1999), are shown by the numbers contained within the white circles.

retroflection. In April 1996, the Amazon Plume can be identified in the sections by warm temperatures (Fig. 13a) and low salinities (Fig. 14a), juxtaposed along the coastline south of 4°N; on careful inspection, this corresponds to the mapping of the surface salinity when the inshore plume is slightly more extensive and closer to the first station of the sections at 45.0°W, 0.5°N (Fig. 10a), than during the other season (Fig. 10b). In September 1995 a surface salinity contrast of −4 (Fig. 14b) and a temperature contrast of +2 °C (Fig. 13b) is observed across the offshore NBC retroflection front at 4°N when the Amazon Plume spreads around to the north of the NBC retroflection. In April 1996 the gradient is reversed with a surface salinity contrast of +3 (Fig. 14a) and a temperature contrast of almost −2 °C (Fig. 13a), because the Amazon Plume is overlaying the NBC retroflection. These Amazon temperature (Fig. 13) and freshwater (Fig. 14) signals are observed down to about 50-m depth. In addition, at 50 m there is a NBC velocity maximum core of 90 cm/s in April 1996 and of 110 cm/s in September 1995 (Bourlès et al., 1999); the retroflection velocity maximum core is 100 cm/s at 80 m in both April 1996 and September 1995 (Bourlès et al., 1999). These flows, essential to the generation of NBC rings, are within tens-of-meters of the edges of the Amazon

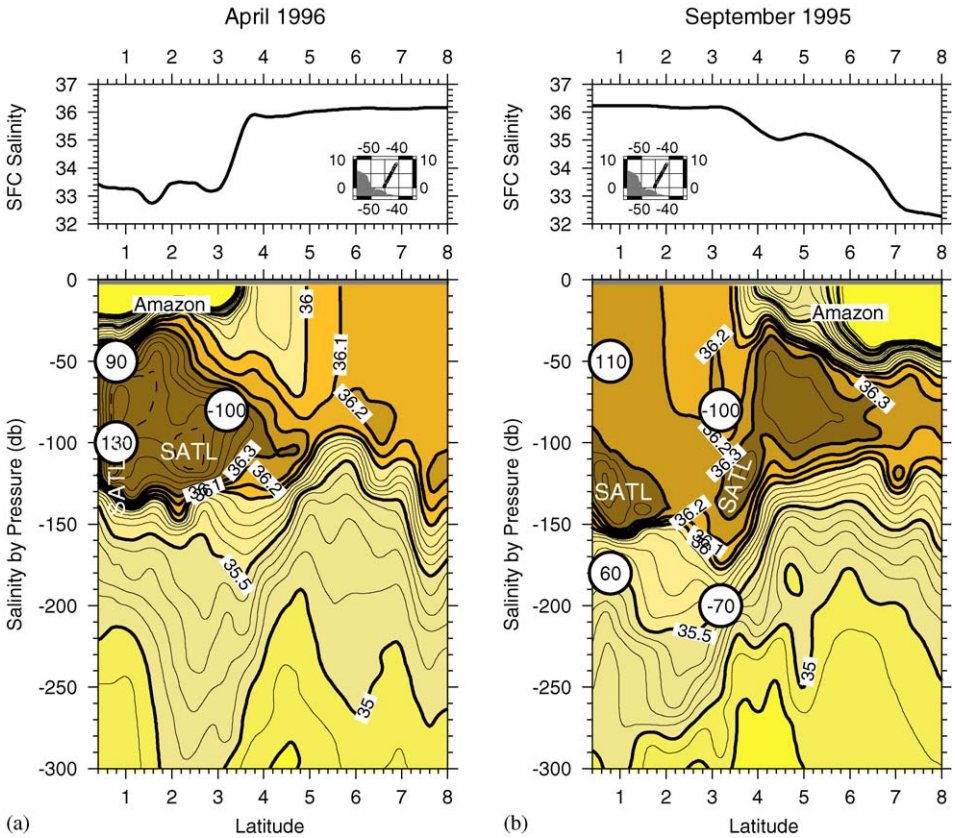

Fig. 14. Surface salinity–latitude plots and salinity–latitude sections for April 1996 (a) and September 1995 (b) obtained as part of the World Ocean Circulation Experiment (described in Bourlès et al., 1999). The locations of the stations are shown in the map insets, crossing the NBC and its retroflection. The low salinities of the Amazon Plume are indicated by the "Amazon" labels and the high salinity water in the NBC retroflection probably coming from the South Atlantic are labeled "SATL". In addition, the magnitude and depth of the NBC retroflection current cores (cm/s), obtained from acoustic doppler current measurements (Bourlès et al., 1999), are shown by the numbers contained within the white circles.

Plume. Consequently, the surface layer characteristics of the rings shed from the NBC retroflection may be influenced by the Amazon Plume and its seasonal variations.

3.6.4. Buoyancy of the Amazon Plume

The fresher and typically warmer surface waters of the Amazon Plume are buoyant relative to the saltier and typically colder surface waters carried by the NBC; for example, in the region just north of the Amazon River delta (stations bounded by 50°W, 48°W, 0°N, 4°N), the average historical surface density is only 1008.3 kg m^{-3} for January–June and 1014.2 kg m^{-3} for July–December, whereas within the NBC (stations bounded by 42°W, 40°W, −4°S, 0°S) the average historical surface density is relatively dense at 1023.0 kg m^{-3} for January–June and 1023.7 kg m^{-3} for July–December.

Normally temperature variations predominately control density changes in the tropical regions, but in the NBC retroflection region the salinity contrasts are so large at the surface due to the freshwater of the Amazon Plume that the effects of salinity variations dominate: at warm temperatures a dynamic height calculation reveals that a 1 decrease in salinity raises the dynamic height about twice as much as a 1 °C increase in

temperature. In September 1995 when the Amazon Plume is north of the retroflection, the contrast in the surface layer across 4°N is −4 for salinity (Fig. 14b) and +2 °C for temperature (Fig. 13b). In April 1996 when the Amazon Plume covers the NBC and retroflection, the contrast in the surface layer across 4°N is +3 for salinity (Fig. 14a) and −2 °C for temperature (Fig. 13a). In both cases the salinity and temperature gradients work in concert, with the salinity effect four times larger. However in April 1996 the dynamic height is increased over the NBC, whereas in September 1995 the dynamic height is increased north of the retroflection due to the different locations of the Amazon Plume. This suggests that the surface dynamics in the region may be influenced by the varying position of the Amazon Plume.

3.7. Surface-intensified NBC rings

In the NBCR experiment, shipboard observations revealed three surface-intensified rings with velocity maximums near the surface (Wilson et al., 2002). The NBCR experiment, in situ observations are used to identify the surface temperature and salinity characteristics of the rings in order to determine the influence of the Amazon River. The rings were surveyed during the first half of the year: two rings during the February 1999 cruise and one ring during the February 2000 cruise. The surface ring temperatures and salinities are consistent with a NBC source. In the straight-forward example from February 1999, the newly formed easternmost ring (Figs. 15c and d; right ring) displays warm surface temperatures and high salinities similar to the temperatures and salinities of the source NBC (Figs. 15c and d; partial ellipse). The surface temperatures of the two other examples are more complicated to interpret, because the NBC and rings were surveyed several months after the rings had been shed and in addition the rings were formed during the low-contrast temperature transition months. In February 1999 the westernmost ring was surveyed, but it had been formed in December 1998, and the ring displays cool surface temperatures consistent with the earlier date of its formation and high surface salinities consistent with the source NBC salinities (Figs. 15c and d). The third surface-intensified ring, surveyed in February 2000, but formed earlier in December 1999, also displays the salty surface salinities of the NBC source (the NBC is narrowly contained against the 200 m contour), but the surface temperatures are relatively warm in this case (Figs. 15e and f).

In the three examples of surface-intensified rings, high salinities are observed across the surfaces of the rings, similar to the salinities across the surface of the NBC. In addition, the three rings display low salinities, between 33.5 and 35.4, just at their outermost edges. This is fresh Amazon Plume water surrounding the rings or else swept up into the edges of the rings and carried along with them as they translate northwestwards towards the Caribbean. With data off the west coast of Barbados, Kelly et al. (2000) correlate episodes of low-salinity water (32.5–34.5), originating from the Amazon River mixing zone, to NBC rings identified by satellite sea level height anomalies. The ring salinity observations shown here (Figs. 15d and f) only reveal low salinities at the edges of the rings implying that there may be alteration of the ring surface characteristics before they reach Barbados. Another possibility is that intermittently rings are generated with Amazon River water completely covering their surfaces; for example, a ring generated from the NBC retroflection in April 1996 (Fig. 14a) when the Amazon Plume completely covered the retroflection could be such a case.

3.8. Thermocline-intensified NBC ring

The only NBCR experiment shipboard observations of a ring from the second half of the year, in November–December 1998, are also the first observations of a thermocline-intensified ring with "almost no detectable surface expression" in velocity (Wilson et al., 2002). The in situ observations are used to identify the surface temperature and salinity characteristics of the ring, in order to determine the influence of the Amazon River. The shipboard velocity observations of the ring in mid-November (first leg of the cruise) and early December (second leg of the cruise) reveal the expected northwestward translation (labeled

circles in Fig. 16) as reported in Wilson et al. (2002). Velocities greater than 1 m/s are observed at the subsurface maximum at 145 m (Fig. 15b, velocity vectors enclosed in dashed and solid circles), dropping to 0.4 m/s above and below the core, at about 50 and 400 m respectively (Wilson et al., 2002). In the satellite SST observations in mid-October 1998, just before the in situ cruise observations, there is a dramatic, nearly 400 km diameter, circular cold anomaly observed (Fig. 16)

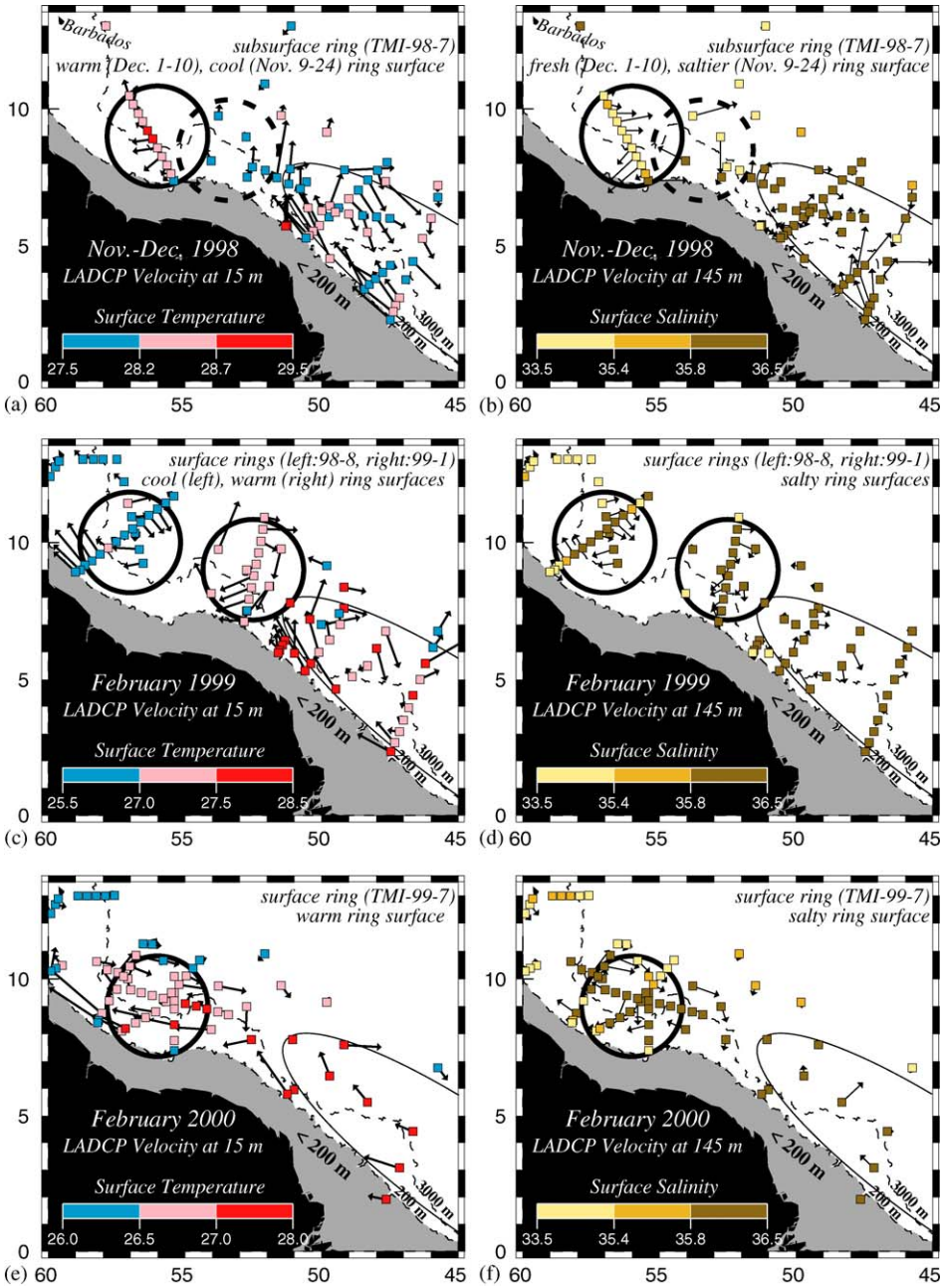

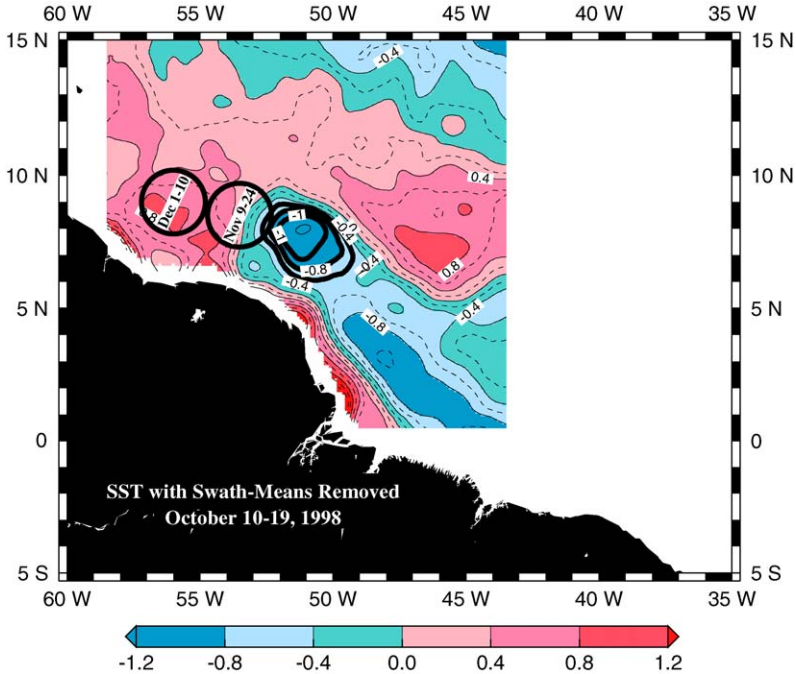

Fig. 16. The anomaly SST image for October 10–19, 1998 smoothed by a 1° by 1° block average; the swath-mean temperature has been removed from each swath and the results averaged to re-construct the image. (After verifying against the 7° by 7° image, this 14° by 14° image is shown here only in order to easily include the complementary cool-anomaly signal of the NBC retroflection region.)

with temperatures 1 °C cooler than the surrounding water in accordance with the prediction of a cold SST ring anomaly for this time of year. In mid-November (during the first leg of the cruise), both the satellite and in situ (Fig. 15a, dashed circle) data also reveal a cold SST anomaly associated with the ring, but by early December (during the second leg of the cruise), more than 500 km downstream, there is no longer a cold SST anomaly associated with the ring in the satellite data, and warmer surface temperatures are observed in the in situ data (Fig. 15a, solid circle). Viewed within satellite SST time series at the location of the current meter mooring, the ring is observed as a small cold SST anomaly in the plain time series (Fig. 2a, TMI-98-7), and as one of the largest cold anomalies in the swath-mean removed time series at nearly the same time and location as the first cruise leg observation of the ring (Fig. 8a, solid circle labeled "7" on November 5, 1998). For additional substantiation of the cold SST ring, the infrared-based SST (Fig. 17) is shown for mid-

Fig. 15. Maps showing the color-coded surface temperatures (a, c, e) and salinities (b, d, f), as well as the scaled acoustic doppler velocity vectors from 15 m (a, c, e) and 145 m (b, d, f) depths, for three NBCR experiment cruises. During the November–December 1998 cruise (a, b), the station data from the thermocline-intensified (i.e. subsurface) ring reveal cool and some saltier surface waters during the first cruise leg (stations within the black dashed circle) consistent with the cool and salty source NBC surface waters (stations following the black partial ellipse), but then warmer and fresher Amazon surface waters during the second cruise leg (stations within the black solid circle) in contrast to the cooler and saltier NBC surface waters. During the February 1999 cruise (c, d), the surface-intensified rings are cool (western ring) and warm (eastern ring) consistent with the NBC seasonal surface temperature change, and both ring surfaces are salty consistent with the salty NBC surface waters. During the February 2000 cruise (e, f), the surface-intensified ring is relatively warm and salty consistent with the warm and salty source NBC surface waters. The three surface-intensified rings also reveal some fresh Amazon water, just at their outermost edges, encasing the salty cores (d, f). On the panels, the corresponding satellite SST "TMI-"ring designation of each shipboard-surveyed ring is noted.

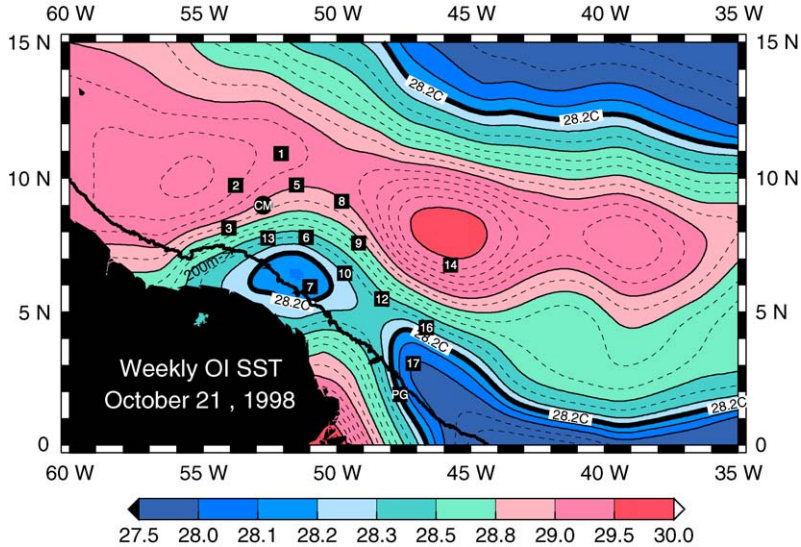

Fig. 17. The SST image for the week centered on October 21, 1998 constructed from optimal interpolation (OI) infrared-derived satellite data smoothed by a 1° by 1° block average. The positions of the inverted echo sounders (numbers), current meter mooring (CM), and shallow pressure gauge (PG) from the NBCR experiment are shown. Note that this image compares well to the microwave-derived anomaly SST image (Fig. 16).

October, and it also reveals the cold circular feature (and NBC retroflection) as did the microwave-based SST image (Fig. 16).

The surface salinity range observed in the November–December 1998 cruise station data is tremendous, from 33.8 to 36.4 (Fig. 15b), and its spatial pattern is consistent with low salinities characteristic of the Amazon Plume (surface salinity <35.8) being swept around and north of the much saltier NBC retroflection (surface salinity >35.8) during this season. As expected, the salinity in the NBC retroflection is high and fairly constant between 36.2 and 36.4, from the surface down to about 100 m (not shown). Initially, in November 9–24, the ring had both high and low salinities (dashed circle Fig. 15b). Then subsequently, in December 1–10, the ring had only low salinities indicative of the fresh Amazon Plume, with all values below 35.8 and as low as 34.6 (solid circle Fig. 15b), consistent with low-salinity ring observations downstream near Barbados (Kelly et al., 2000). During this time of year low-salinity Amazon Plume water is historically observed throughout the region (Fig. 10b), including as far as Barbados (approximately located at 59°W, 13°N). Perhaps, in this case, the final low salinities of the ring are due to weak ring rotation in the surface layer, resulting in source NBC characteristics diluted by mixing with, or flooding by, the surrounding low salinities of the Amazon Plume. In addition, surface dynamics due to the buoyant Amazon Plume lying directly in the pathway of the relatively dense upper layer of the NBC ring may be involved.

The surface layer characteristics of the rings shed from the NBC retroflection reveal varying influence of the Amazon Plume. Consequently, the Amazon River freshwater plume may have an effect in the region, not only as an ocean-atmosphere vertical-barrier (Pailler et al., 1999), but as oceanic horizontal-barrier seasonally introducing buoyancy to the surface layer. In addition, note that the SSTs in both the ring translation corridor and in the NBC steadily decrease over the 1998–2002, 5-year period (Fig. 2c). This continually reduces the average intensity and surface area that the NBC retroflection region contributes to the tropical Western Hemisphere warm pool,

defined by SSTs greater than 28.5 °C and associated with increased tropical convection and the annual development of tropical storms and hurricanes (Wang and Enfield, 2001). Because the Amazon River plume and the NBC retroflection and ring shedding are oceanic forces modulating the SST in the NBC retroflection region, their seasonal and interannual variability may impact the tropical Western Hemisphere warm pool.

4. Conclusions

Five years of satellite SST measurements from the cloud penetrating TRMM Microwave Imager are used to study the shedding of rings at the retroflection of the NBC in the western equatorial Atlantic. In the images and time series the rings are observed to carry the SST characteristics of the NBC retroflection region as they translate northwest in the ring corridor towards the Caribbean. Significantly, the NBC rings are shown to carry a warm (cold) SST anomaly in the first (second) half of the year relative to the regional SSTs surrounding the rings. In all, seven or eight SST anomalies are identified per year in the ring translation corridor revealing warm (cold) SST rings passing by in the first (second) half of the year. The in situ measurements of the NBCR experiment are used to confirm the results for a 1.6 year time period: The timing of the rings observed in the NBCR experiment directly correlates to the timing of the observed warm (cold) SST anomalies during the first (second) half of the year. The temperature contrasts are influenced by the discharge of the Amazon River, the largest in the world, which spreads fresh and warm surface waters directly into the NBC ring generation region.

Historical in situ salinity data highlight the stark surface salinity contrast between the high-salinity NBC retroflection and the low-salinity Amazon River plume. In August, 2–3 months after the maximum Amazon River discharge, the Amazon Plume completely surrounds the NBC retroflection on the west and the north. The surface layer characteristics of the rings shed from the NBC retroflection reveal varying influence of the Amazon Plume. Of the four rings surveyed in the NBCR experiment, Amazon Plume water is found only on the edges of the three surface-intensified rings, whereas Amazon Plume water completely covers the surface layer of the one thermocline-intensified ring. The maximum current cores of the NBC and retroflection are observed within tens-of-meters of the edges of the Amazon Plume, either overlaying or adjacent to the current cores. As the fresher and typically warmer surface waters associated with the Amazon Plume are buoyant relative to the saltier and typically colder surface waters carried by the NBC, the varying position of the Amazon Plume may seasonally influence the surface dynamics in the region.

Acknowledgements

This research was supported by the US National Science Foundation, grant OCE9732389. The author would like to express gratitude to the science members and crew of the R/V *Seward Johnson* for the success of the NBCR experiment, to S. Garzoli and G. Goni for thoughtful, productive scientific discussions, and to B. Bourlès for drawing attention to the temperature signal of the Amazon Plume. The TRMM data and images are produced by Remote Sensing Systems and sponsored by NASA's Earth Science Information Partnerships (ESIP): a federation of information sites for Earth Science; and by NASA's TRMM Science Team.

References

Bourlès, B., Gouriou, Y., Chuchla, R., 1999. On the circulation in the upper layer of the western equatorial Atlantic. Journal of Geophysical Research 104, 21151–21170.

Fratantoni, D.M., Glickson, D.A., 2002. North Brazil current ring generation and evolution observed with SeaWiFS. Journal of Physical Oceanography 32, 1058–1074.

Ganachaud, A., Wunsch, C., 2000. Improved estimates of global ocean circulation, heat transport and mixing from hydrographic data. Nature 408, 453–456.

Garraffo, Z.D., Johns, W.E., Chassignet, E.P., Goni, G.J., 2003. North Brazil Current rings and transport of southern waters in a high resolution numerical simulation of the North Atlantic. In: Goni, G.J., Malanotte-Rizzoli, P. (Eds.), Interhemispheric Water Exchange in the Atlantic Ocean.

Elsevier Oceanographic Series, vol. 68. pp. 375–409 (ISBN 0-444-51267-5).

Garzoli, S.L., Ffield, A., Yao, Q., 2003. North Brazil Current rings and the variability in the latitude of retroflection. In: Goni, G. J., Malanotte-Rizzoli, P. (Eds.), Interhemispheric Water Exchange in the Atlantic Ocean. Elsevier Oceanographic Series, vol. 68. pp. 357–373 (ISBN 0-444-51267-5).

Garzoli, S.L., Ffield, A., Johns, W.E., Yao, Q., 2004. North Brazil Current retroflection and transports. Journal of Geophysical Research 109, C01013 (doi:10.1029/2003JC001775).

Goni, G.J., Johns, W.E., 2003. Synoptic study of warm rings in the North Brazil Current retroflection region using satellite altimeter data. In: Goni, G.J., Malanotte-Rizzoli, P. (Eds.), Interhemispheric Water Exchange in the Atlantic Ocean. Elsevier Oceanographic Series, vol. 68. pp. 335–356 (ISBN 0-444-51267-5).

Hellweger, F.L., Gordon, A.L., 2002. Tracing Amazon River water into the Caribbean Sea. Journal of Marine Research 60, 537–549.

Jochum, M., Malanotte-Rizzoli, P., 2003. On the generation of North Brazil Current Rings. Journal of Marine Research 61, 147–173.

Johns, W.E., Lee, T.N., Schott, F.A., Zantopp, R.J., Evans, R.H., 1990. The North Brazil current retroflection: seasonal structure and eddy variability. Journal of Geophysical Research 95, 22103–22120.

Johns, W.E., Lee, T.N., Beardsley, R.C., Candela, J., Limeburner, R., Castro, B., 1998. Annual cycle and variability of the North Brazil current. Journal of Physical Oceanography 28, 103–128.

Johns, W.E., Zantopp, R.J., Goni, G.J., 2003. Cross-gyre transport by North Brazil Current rings. In: Goni, G.J., Malanotte-Rizzoli, P. (Eds.), Interhemispheric Water Exchange in the Atlantic Ocean. Elsevier Oceanographic Series, vol. 68. pp. 411–441 (ISBN 0-444-51267-5).

Kelly, P.S., Lwiza, K.M.M., Cowen, R.K., Goni, G.J., 2000. Low-salinity pools at Barbados, West Indies: their origin, frequency, and variability. Journal of Geophysical Research 105, 19699–19708.

Lentz, S.J., 1995. Seasonal variations in the horizontal structure of the Amazon Plume inferred from historical hydrographic data. Journal of Geophysical Research 100, 2391–2400.

Ma, H., 1996. The dynamics of North Brazil Current retroflection eddies. Journal of Marine Research 54, 35–53.

Metcalf, W.G., 1968. Shallow currents along the northeastern coast of South America. Journal of Marine Research 26, 232–243.

Nof, D., 1996. Why are rings regularly shed in the western equatorial Atlantic but not in the western Pacific? Progress in Oceanography 38, 417–451.

Nof, D., Pichevin, T., 1996. The retroflection paradox. Journal of Physical Oceanography 26, 2344–2358.

Ou, H.W., 1989. Why does the Amazon water flow to the North after its discharge? Journal of Physical Oceanography 19, 1102–1107.

Pailler, K., Bourlès, B., Gouriou, Y., 1999. The Barrier layer in the Western tropical Atlantic Ocean. Geophysical Research Letters 26, 2069–2072.

Perry, G.D., Duffy, P.B., Miller, N.L., 1996. An extended data set of river discharges for validation of general circulation models. Journal of Geophysical Research 101, 21339–21349.

Schott, F.A., Fischer, J., Stramma, L., 1998. Transports and pathways of the upper-layer circulation in the western tropical Atlantic. Journal of Physical Oceanography 28, 1904–1928.

Stramma, L., Schott, F., 1996. Western equatorial circulation and interhemispheric exchange. In: Krauss, W. (Ed.), The Warmwatersphere of the North Atlantic Ocean. Gebruder Borntraeger, Berlin, pp. 195–227.

Wang, C., Enfield, D.B., 2001. The tropical Western Hemisphere warm pool. Geophysical Research Letters 28, 1635–1638.

Wentz, F.J., Meissner, T., 2000. Algorithm Theoretical Basis Document (ATBD), Version 2, AMSR Ocean Algorithm. RSS Tech. Proposal 121599A-1, Remote Sensing Systems, Santa Rosa, CA, 59pp.

Wilson, W.D., Johns, E., Molinari, R.L., 1994. Upper layer circulation in the western tropical North Atlantic Ocean during August 1989. Journal of Geophysical Research 99, 22513–22523.

Wilson, D.W., Johns, W.E., Garzoli, S.L., 2002. Velocity structure of North Brazil Current rings. Geophysical Research Letters 29, 114 (10.1029/2001GL013869).